

A BIFURCATION ANALYSIS OF HIGH-TEMPERATURE IGNITION OF $\text{H}_2\text{-O}_2$ DIFFUSION FLAMES

ANTONIO L. SÁNCHEZ

*Center for Energy and Combustion Research
University of California–San Diego, La Jolla, CA 92093-0310, USA*

AMABLE LIÑÁN

*Universidad Politécnica de Madrid, E. T. S. I. Aeronauticos
Plaza Cardenal Cisneros 3, 28040 Madrid, Spain*

AND

FORMAN A. WILLIAMS

*Center for Energy and Combustion Research
University of California–San Diego, La Jolla, CA 92093-0310, USA*

The form of the ignition branch for steady, counterflow, hydrogen-oxygen diffusion flames, with dilution permitted in both streams, is investigated for two-step reduced chemistry by methods of bifurcation theory. Attention is restricted to fuel-stream temperatures less than or equal to the oxidizer-stream temperature T_∞ and to T_∞ larger than or of the order of the crossover temperature T_c at which the rates of production and consumption of H atoms are equal. Two types of solutions are identified, a frozen solution that always exists in this kinetic approximation because all rates are proportional to the concentration of the intermediate H atom, and an ignited solution, represented by a branch of the curve giving the maximum H concentration in terms of a Damköhler number constructed from the strain rate and the rate of the branching step $\text{H} + \text{O}_2 \rightarrow \text{OH} + \text{O}$. For $T_\infty > T_c$, the latter bifurcates from the frozen solution if the Damköhler number is increased to a critical value. For T_∞ larger than a value $T_s > T_c$, the effects of chemical heat release are small, and ignition is always gradual in the sense that the limiting ignited-branch slope is positive (supercritical bifurcation) and there is no S curve. For T_∞ in the range $T_c < T_\infty < T_s$, the heat release associated with the radical-consumption step causes the limiting ignition-branch slope to become negative (subcritical bifurcation), producing abrupt ignition which leads to an S curve. For values of T_∞ below crossover, the ignited branch appears as a C-shaped curve unconnected to the frozen solution. The method of analysis introduced here offers a first step toward analytical description of nonpremixed $\text{H}_2\text{-O}_2$ autoignition.

Introduction

Because of interest in applications such as aerospace propulsion, considerable attention has been given in the literature to the study of ignition of hydrogen-oxygen mixtures. Treviño [1] investigated ignition in an isochoric, adiabatic, homogeneous reactor and systematically reduced the well-known detailed reaction mechanism [2–5] to small numbers of global steps for different pressure and temperature regimes. He found that the ignition process is strongly dependent upon the initial temperature of the mixture. A relevant parameter in the description of $\text{H}_2\text{-O}_2$ ignition is the so-called crossover temperature T_c , the temperature at which the rates of production and consumption of H radicals are equal. The two determinant reaction rates are those of the

chain-branching reaction $\text{H} + \text{O}_2 \rightarrow \text{OH} + \text{O}$ and the chain-terminating reaction $\text{H} + \text{O}_2 + \text{M} \rightarrow \text{HO}_2 + \text{M}$. For initial temperatures on the order of T_c , Treviño [1] deduced a five-step mechanism, which can be further simplified by neglecting the initiation step $\text{H}_2 + \text{O}_2 \rightarrow \text{HO}_2 + \text{H}$ and assuming that the hydroperoxyl radical HO_2 is in steady state [6,7]. Reduced chemistry of as few as two steps has been proposed for high-temperature ignition above crossover [8].

Autoignition in practical systems generally occurs during mixing of cool hydrogen with a hot oxidizing gas, leading to the establishment of $\text{H}_2\text{-O}_2$ diffusion flames. In such nonpremixed environments, some details of the chemistry may differ from that in homogeneous systems because of complications associated with H_2 diffusion into the O_2 inert mixture.

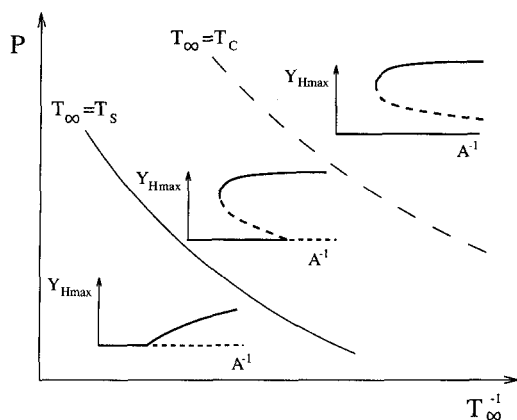


FIG. 1. Ignition behaviors present in high-temperature ignition of $\text{H}_2\text{-O}_2$ diffusion flames.

While numerous investigations have been reported on $\text{H}_2\text{-O}_2$ ignition histories in homogeneous systems, only a few studies of ignition of $\text{H}_2\text{-O}_2$ diffusion flames are available [8,9], and they are purely numerical* and are restricted to steady flows so that ignition times cannot be determined, although critical conditions needed for ignition to occur are obtained. Except for one study [10] including model branched-chain kinetics for a premixed system exposed to a hot inert gas, previously published analytical investigations of the ignition branch of the S curve have been restricted to one-step chemistry.

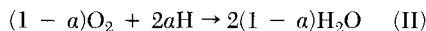
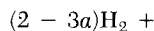
The main objective of the present paper is to apply the reduced kinetic mechanism derived by Treviño [1] to study the ignition of strained diffusion flames. Steady counterflow systems are addressed, following preliminary ideas developed [11] in considering coflow mixing layers. To simplify the analysis, an inviscid potential solution is adopted to describe the flow field. Although the model retains the physical characteristics of the problem, a more thorough description of the flow field is required if quantitative agreement with numerical results is to be obtained.

For high-temperature $\text{H}_2\text{-O}_2$ diffusion flames, Fig. 1 summarizes the different shapes that the ignition curve may exhibit in a plot of the maximum radical concentration as a function of the inverse of the strain rate. For oxidizer-stream temperatures above T_c , the ignited branch bifurcates from the frozen solution at a finite value of the strain rate. The occurrence of ignition as a bifurcation as opposed to a smooth turning point as in conventional one-step asymptotic analyses [12] is a consequence of the autocatalytic character of the kinetic mechanism em-

ployed. A limiting temperature $T_s > T_c$ that determines the criticality of the bifurcation will be identified. Above this temperature, the chemical heat release is negligibly small, and a progressive transition from frozen flow to the equilibrium diffusion-flame solution takes place. We shall show that, for stream temperatures below T_s , the exothermicity associated with the radical recombination changes the character of the solution, and an S-shaped curve more typical of diffusion flames is reproduced. As T_c is approached, the strain rate at which ignition occurs decreases, becoming zero at crossover. If the initiation step is neglected in the kinetic mechanism, no chain-branched autoignition is possible below crossover, and the ignited and frozen solutions are unconnected. The ignition behavior shown in Fig. 1 is in qualitative agreement with the numerical results available [8,9].

Kinetic Mechanism and Formulation

The high-temperature ignition of $\text{H}_2\text{-O}_2$ mixtures can be described [1] by the reduced kinetic mechanism $\text{H}_2 + \text{O}_2 \rightarrow \text{HO}_2 + \text{H}$, $3\text{H}_2 + \text{O}_2 \rightarrow 2\text{H} + 2\text{H}_2\text{O}$, $\text{H} + \text{O}_2 + \text{M} \rightarrow \text{HO}_2 + \text{M}$, $2\text{H}_2 + \text{HO}_2 \rightarrow 2\text{H}_2\text{O} + \text{H}$, $\text{HO}_2 + \text{H} \rightarrow \text{H}_2 + \text{O}_2$, where O and OH are assumed to be in steady state. Although the first of these five steps is important at early times during initiation, once trace amounts of radicals are present, its influence becomes negligible, and we neglect it here. A steady state for hydroperoxyl is an excellent approximation [6–8], and since this radical appears in four of the five steps, its steady state reduces the chemistry to a two-step mechanism. If $(a^{-1} - 1)$ denotes the ratio of the rate of the elementary step $\text{HO}_2 + \text{H} \rightarrow \text{OH} + \text{OH}$ to that of the step $\text{HO}_2 + \text{H} \rightarrow \text{H}_2 + \text{O}_2$, then this two-step mechanism is



with rates given, respectively, by those of the elementary reactions $\text{H} + \text{O}_2 \rightarrow \text{OH} + \text{O}$ and $\text{H} + \text{O}_2 + \text{M} \rightarrow \text{HO}_2 + \text{M}$. The specific reaction-rate constants for these two elementary reactions will be denoted by k_1 and k_2 , respectively. This same two-step description has been employed in a recent analysis of the premixed H_2 -air flame [13] and elsewhere [6]. From the latest data available [8], it can be shown that $a \approx 1/6$ over the temperature range of interest. Thus, only a small fraction of the HO_2 produced is consumed by $\text{HO}_2 + \text{H} \rightarrow \text{H}_2 + \text{O}_2$, partially attenuating, therefore, the chain-terminating effect of reaction II. The overall step I is weakly exothermic, its heat of reaction being roughly an order of magnitude

*An exception is a recent study by activation-energy asymptotics (S. R. Lee and C. K. Law, *Combust. Sci. Technol.*, to appear, 1994) that does not address bifurcation theory.

smaller than that corresponding to II. For values of the mixture temperature sufficiently above T_c , production of HO₂ can be neglected entirely, and the kinetic mechanism reduces to the overall step I. The ignition process is then a typical chain-branching explosion with a fairly small heat release effect. As the temperature of the streams approaches T_c , step II gains importance. The ignition is still characterized as a chain-branching explosion, but now the exothermicity of II as well as its chain-terminating effect play an increasingly important role in the ignition process. Both behaviors will be analyzed in this paper.

Attention will be restricted to stagnation-point counterflow of H₂ and O₂, dilution with an inert being permitted in both feed streams. We shall assume, for the sake of simplicity, that the strain rate, density, specific heat, and transport coefficients are constant; these assumptions are readily removed through suitable well-known transformations. The equations that describe the flow are then given by

$$\zeta \frac{\partial y_H}{\partial \zeta} + \frac{\partial^2 y_H}{\partial \zeta^2} = -A[\exp(\beta_1 \theta) - \gamma] y_{O_2} y_H \quad (1)$$

$$\zeta \frac{\partial y_{O_2}}{\partial \zeta} + \frac{L_H}{L_{O_2}} \frac{\partial^2 y_{O_2}}{\partial \zeta^2} = sA[\exp(\beta_1 \theta) + (1 - a)\gamma/a] y_{O_2} y_H \quad (2)$$

$$\zeta \frac{\partial \theta}{\partial \zeta} + L_H \frac{\partial^2 \theta}{\partial \zeta^2} = -A[q_I \exp(\beta_1 \theta) + q_{II}\gamma/a] y_{O_2} y_H \quad (3)$$

and

$$\zeta \frac{\partial y_{H_2}}{\partial \zeta} + \frac{L_H}{L_{H_2}} \frac{\partial^2 y_{H_2}}{\partial \zeta^2} = 3A[\exp(\beta_1 \theta) + (2 - 3a)\gamma/(3a)] y_{O_2} y_H \quad (4)$$

where the nondimensional variables are defined as

$$\begin{aligned} \zeta &= y \left(\frac{L_H A}{D} \right)^{1/2}, & y_H &= \frac{Y_H}{Y_{H_2-\infty}}, \\ y_{O_2} &= \frac{Y_{O_2}}{Y_{O_2\infty}}, & \theta &= \frac{T - T_\infty}{T_\infty}, & y_{H_2} &= \frac{Y_{H_2}}{Y_{H_2-\infty}}, \\ A &= \frac{2B_1 \exp(-\beta_1) \rho Y_{O_2\infty}}{W_{O_2} A}, & s &= \frac{W_{O_2}}{W_{H_2}} \frac{Y_{H_2-\infty}}{Y_{O_2\infty}}, \\ q_i &= \frac{q'_i}{c_p T_\infty} \frac{Y_{H_2-\infty}}{W_{H_2}}, & \gamma &= \frac{A_2}{A_1} \frac{P \exp(\beta_1) a}{R^0 T_\infty^{(1+n_1-n_2)}}. \end{aligned} \quad (5)$$

The boundary conditions for the above equations are $y_H \rightarrow 0$, $y_{H_2} \rightarrow 1$, $y_{O_2} \rightarrow 0$, and $\theta \rightarrow \theta_{-\infty} \equiv (T_{-\infty} - T_\infty)/T_\infty$ as $\zeta \rightarrow -\infty$ and $y_H \rightarrow 0$, $y_{H_2} \rightarrow 0$, $y_{O_2} \rightarrow 1$, and $\theta \rightarrow 0$ as $\zeta \rightarrow +\infty$.

Here y is the transverse coordinate with origin at the dividing fluid surface, T is the temperature, and Y_H , Y_{H_2} , and Y_{O_2} are the mass fractions of atomic hydrogen, molecular hydrogen, and oxygen, whose Lewis numbers are denoted by L_H , L_{H_2} , and L_{O_2} . Hydrogen is approaching from $-\infty$ with mass fraction $Y_{H_2-\infty}$ and temperature $T_{-\infty}$, while the oxidizer flows from $+\infty$, where the oxygen mass fraction is $Y_{O_2\infty}$ and the temperature is T_∞ . The thermal diffusivity of the mixture is given by $D = \lambda/(\rho c_p)$, where λ is the thermal conductivity, ρ is the fluid density, and c_p is the specific heat at constant pressure, all taken to be constant. The reaction-rate constant, $k_1 = A_1 T^{n_1} \exp(-E_1/R^0 T)$, has been approximated by $k_1 = B_1 \exp(-\beta_1) \exp(\beta_1 \theta)$, where B_1 is a new frequency factor given by $B_1 = A_1 T_\infty^{n_1}$ and β_1 is the nondimensional activation temperature $\beta_1 = E_1/(R^0 T_\infty)$. The variation of $k_2 C_M$ with temperature has been neglected, so that $k_2 C_M = A_2 T_\infty^{n_2} P/(R^0 T_\infty)$, C_M being the efficiency-weighted sum of third-body concentrations. Updated values of the reaction-rate constants in mol/cm³, s⁻¹, K, and cal/mol are [8] $A_1 = 3.52 \times 10^{16}$, $A_2 = 6.76 \times 10^{19}$, $E_1 = 17,070$, $n_1 = -0.7$, and $n_2 = -1.42$. The W 's are molecular weights, A is the constant strain rate, P is the uniform pressure across the mixing layer, and q'_i is the heat release associated with overall step i . Six parameters appear in the equations, namely, A , s , $\theta_{-\infty}$, γ , q_I , and q_{II} , besides the constant a , the Lewis numbers, and the activation-energy parameter β_1 . Here A is an appropriate nondimensional Damköhler number, s is an oxygen-to-fuel mass ratio corresponding to the approaching streams, $\theta_{-\infty}$ accounts for the temperature difference between the streams, γ is the ratio of consumption to production rates of H radicals by the two competing reactions evaluated at $T = T_\infty$, and q_I and q_{II} are the nondimensional heats of reaction associated with each global step. The use of T_∞ as the relevant characteristic temperature is dictated later by the location of the reaction region.

The problem defined by Eqs. (1) through (4) admits two types of solutions. The first corresponds to the trivial solution $y_H = 0$, $y_{O_2} = y_{O_2f}$, $\theta = \theta_f$, $y_{H_2} = y_{H_2f}$, where y_{O_2f} , θ_f , and y_{H_2f} are the frozen profiles corresponding to y_{O_2} , θ , and y_{H_2} , respectively. These solutions, which exist for all values of A , are given by

$$\begin{aligned} y_{O_2f} &= \left[1 - \frac{1}{2} \operatorname{erfc}(\zeta/\sqrt{2L_H}) \right], \\ \theta_f &= \frac{\theta_{-\infty}}{2} \operatorname{erfc}(\zeta/\sqrt{2L_H}), & y_{H_2f} &= \frac{1}{2} \operatorname{erfc}(\zeta/\sqrt{2}). \end{aligned} \quad (6)$$

For Δ sufficiently large, another solution exists as well. Before studying this ignited solution, further constraints, arising from the physics of the problem, must be identified.

A first constraint is that the solution must give positive values of y_H everywhere in the mixing layer. This imposes an upper limit to the range of Δ for which a solution can be found for a given value of y_H , termed $y_{H_{\max}}$. A second constraint is that y_{H_2} must be positive for the validity of the two-step kinetic scheme. As a consequence of the reduced mechanism adopted, y_{H_2} does not appear in the chemical production terms on the right-hand sides of Eqs. (1) through (4). Therefore, Eqs. (1) through (3) can be solved separately, and y_{H_2} can be obtained afterward from Eq. (4). When y_{H_2} is calculated in this way, it is found that there exists a value of ζ , termed ζ_d , such that $y_{H_2} < 0$ for $\zeta > \zeta_d$; ζ_d decreases with increasing $y_{H_{\max}}$. To avoid negative y_{H_2} , the chemical-reaction model must be modified at sufficiently large ζ to account for H_2 depletion. The kinetic mechanism adopted holds only for values of ζ such that the resultant mixture is not too fuel lean, and for large values of ζ , where y_{H_2} is very small, this mechanism fails and should be replaced by an alternative developed by Treviño and Liñán [11] for lean mixtures. The revised formulation would result in a profile of H_2 smoothly decaying to zero as ζ increases. The approach employed here is simpler in that we assume that the kinetic mechanism for lean and stoichiometric mixtures holds as long as $y_{H_2} > 0$, and for values of ζ larger than the depletion point ζ_d , the chemical reaction is completely frozen. This approximation is motivated by the low rate of the alternative path, controlled by $O + H_2 \rightarrow OH + H$, in the region $\zeta > \zeta_d$ where the concentrations of both H_2 and the radicals are very small. The freezing of the reaction can be introduced formally into Eqs. (1) through (4) by multiplying the chemical production term by a Heaviside function $H(\zeta - \zeta_d)$. The problem defined in this form with the boundary conditions previously stated has a unique nontrivial solution for a given value of the depletion point ζ_d .

Linear and Weakly Nonlinear Analysis for $T_\infty \geq T_c$

The value of the critical Damköhler number for ignition of the autocatalytic reaction, Δ_c , as well as the slope of the bifurcated ignited branch, can be obtained by solving the linearized version of Eqs. (1) through (3) and the equations for the second perturbation. We consider first the problem in which both streams have the same temperature, $\theta_{-\infty} = 0$, and assume that $L_{O_2} = 1$. Since near the bifurcation point $y_{H_{\max}} \ll 1$ and depletion of H_2 occurs far from the stagnation plane, a further simplification can be introduced. For large values of ζ and $\zeta < \zeta_d$, Eq. (1)

admits two different types of solutions, whose behaviors as $\zeta \rightarrow \infty$ are given by $\zeta^{[\Delta(1-\gamma)-1]} \exp(-\zeta^2/2)$ and $\zeta^{-\Delta(1-\gamma)}$, respectively. For values of ζ beyond the depletion point, the solution to Eq. (1) is proportional to $\text{erfc}(\zeta/\sqrt{2})$. Matching of the values of the frozen and nonfrozen solutions and their slopes at $\zeta = \zeta_d$ reveals that solutions with algebraic decay are not admissible for $\zeta < \zeta_d$. Therefore, to find the solution for the ignited branch for small values of $y_{H_{\max}}$, we can ignore Eq. (4) and replace the Heaviside function on the right-hand side of Eqs. (1) through (3) by the requirements of exponential decay of y_H as $\zeta \rightarrow \infty$ and $y_H > 0$ throughout the mixing layer. It is worth observing that use of this modification causes the solution in the vicinity of the bifurcation point to be independent of the H_2 diffusion coefficient; i.e., the results are independent of the value of L_{H_2} .

For values of $y_{H_{\max}} = \varepsilon \ll 1$, we can introduce the asymptotic expansions

$$\begin{aligned}\Delta &= \phi_1 \Delta_0 + \varepsilon s \phi_1^2 \phi_2 \Delta_1, \\ y_H &= \varepsilon y_{H0} + \varepsilon^2 s \phi_1 \phi_2 y_{H1} \\ y_{O_2} &= y_{O2f} - \varepsilon s \phi_1 \phi_2 y_{O20}, \\ \theta &= \varepsilon \phi_1 (q_1 + q_{11} \gamma / a) \theta_0\end{aligned}\quad (7)$$

where $\phi_1 = (1 - \gamma)^{-1}$, $\phi_2 = [1 + (1 - a)\gamma/a]$, and y_{O2f} is given by Eq. (6). Here y_{H0} is scaled so that its maximum value is unity. Introducing the above expansions into Eqs. (1) through (3) and collecting terms with the same power of ε , we obtain the equations

$$\zeta \frac{\partial y_{H0}}{\partial \zeta} + \frac{\partial^2 y_{H0}}{\partial \zeta^2} = -\Delta_0 y_{O2f} y_{H0} \quad (8)$$

$$\zeta \frac{\partial y_{O20}}{\partial \zeta} + L_H \frac{\partial^2 y_{O20}}{\partial \zeta^2} = -\Delta_0 y_{O2f} y_{H0} \quad (9)$$

and

$$\zeta \frac{\partial y_{H1}}{\partial \zeta} + \frac{\partial^2 y_{H1}}{\partial \zeta^2} = -\Delta_0 y_{O2f} y_{H1}$$

$$+ \Delta_0 [1 - \Omega y_{O2f}] y_{O20} y_{H0} - \Delta_1 y_{O2f} y_{H0} \quad (10)$$

with boundary conditions that y_{H0} , y_{O20} , and y_{H1} approach zero as $\zeta \rightarrow \pm \infty$. The equation that determines θ_0 is simply $\theta_0 = y_{O20}$. The form of the expansions in Eq. (7) is such that the only parameters left in Eqs. (8) through (10) are L_H and $\Omega = \beta_1 (q_1 + q_{11} \gamma / a) \phi_1 / (s \phi_2)$.

Critical Damköhler Number for Ignition:

For a given value of the Lewis number of the fuel, Eq. (8) with the stated boundary and nonnegativity

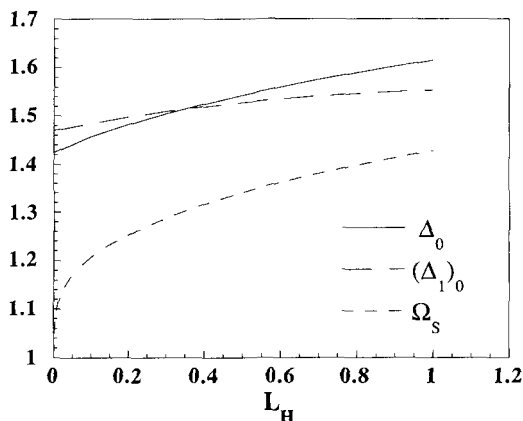


FIG. 2. Variation of the critical Damköhler number, slope of the bifurcation, and criticality condition parameter with the Lewis number of hydrogen.

conditions represents an eigenvalue problem and has a nontrivial solution for only one value of Δ_0 . The results obtained for different values of L_H are shown in Fig. 2. The critical Damköhler number for ignition is then given by $\Delta_c = \Delta_0/(1 - \gamma)$. To understand the significance of this result, one must recall that the Damköhler number Δ is constructed from the strain rate and the rate of the branching step $H + O_2 \rightarrow OH + O$, while $\gamma > 1$ for $T_\infty < T_c$, is the ratio of the rate of radical consumption to that of radical production. Therefore, the quantity $(1 - \gamma)\Delta_c$, a constant of order unity for a given value of L_H , represents the ratio of the characteristic strain time to the characteristic chemical time of the two-step kinetic mechanism necessary for ignition to occur. As T_∞ approaches T_c , the chain-terminating character of step II causes the value of γ to increase, which corresponds to an increment of the characteristic chemical time of radical production. Therefore, the lower the temperature is, the lower is the value of the critical strain rate at ignition. A chain-branching explosion is no longer possible for T_∞ below the crossover temperature at which $\gamma = 1$, and the critical Damköhler number becomes infinite. For $T_\infty < T_c$, the frozen and ignited branches are unconnected, and the latter becomes a C-shaped curve standing above $y_{H_{max}} = 0$. Connection between both branches can be recovered if the initiation step $H_2 + O_2 \rightarrow HO_2 + H$ is retained in the kinetic scheme. For sufficiently large values of the Damköhler number, the characteristic residence time A^{-1} becomes a large quantity of the order of the chemical time associated with the initiation step, and production of H radicals by this step is no longer negligible. Ignition in this case is governed by this step that provides a smooth connecting branch between the frozen and ignited curves. For even lower temperatures, ignition occurs as a ther-

mal-runaway process governed by a different kinetic mechanism [1,7].

Bifurcation Character:

The parameter Δ_1 , which gives the slope of the bifurcated branch, can be obtained by integrating Eq. (10) or by using the solvability condition

$$\int_{-\infty}^{\infty} y_{H_0}^2 [\Delta_0 y_{O_2} (1 - \Omega y_{O_2 f}) - \Delta_1 y_{O_2 f}] \exp(\zeta^2/2) d\zeta = 0 \quad (11)$$

which can be solved for Δ_1 to give $\Delta_1 = (1 - \Omega/\Omega_s)(\Delta_1)_0$, where

$$\Omega_s = \frac{\int_{-\infty}^{\infty} y_{O_2} y_{H_0}^2 \exp(\zeta^2/2) d\zeta}{\int_{-\infty}^{\infty} y_{O_2 f} y_{O_2} y_{H_0}^2 \exp(\zeta^2/2) d\zeta} \quad (12)$$

and

$$(\Delta_1)_0 = \frac{\int_{-\infty}^{\infty} y_{O_2} y_{H_0}^2 \exp(\zeta^2/2) d\zeta}{\int_{-\infty}^{\infty} y_{O_2 f} y_{H_0}^2 \exp(\zeta^2/2) d\zeta} \Delta_0. \quad (13)$$

The results of these integrations for different values of the Lewis number of the fuel are shown in Fig. 2.

The criticality of the bifurcation is governed by the parameter Ω that measures the counteracting effects of oxygen consumption and temperature increase resulting from heat release. The behavior of the ignition branch can be explained by considering the right-hand side of Eq. (1). When Ω is larger than Ω_s , the effect of temperature rise dominates the ignition process through the exponential term $\exp(\beta_1 \theta)$, causing the Damköhler number to decrease as $y_{H_{max}}$ increases, resulting in a subcritical bifurcation. On the other hand, for small values of Ω , corresponding to large T_∞ and small $Y_{O_{2\infty}}$, the effect of oxygen consumption takes over, giving an overall decreasing $[\exp(\beta_1 \theta) - \gamma]y_{O_2}$ term. To balance this effect, as $y_{H_{max}}$ increases Δ must increase, and the bifurcated branch becomes supercritical.

The equation $\Omega = \Omega_s$ determines a limiting temperature T_s that clearly separates abrupt ignition behaviors from smooth transitions to the diffusion-flame solution. For values of T_∞ far above the crossover temperature, γ becomes negligibly small, and Ω reduces to $\beta_1 q_1/s$. Numerical evaluation of this expression reveals that the heat release associated with step I is too small to change the character of the bifurcation, so that it remains supercritical as long as the production of HO_2 is negligible. Since $q_{II}/a \gg q_I$, as T_∞ decreases the value of Ω increases signifi-

cantly, and a subcritical character is achieved somewhat above crossover, i.e., $T_s > T_c$. The curves characterizing the ignition behavior sketched in Fig. 1 can be plotted for a given value of $Y_{O_{2s}}$ by using the equations $\gamma = 1$ and $\Omega = \Omega_s$. Typically, as P varies from 10^{-1} to 10^2 atm, T_c varies from 800 to 1400 K, and $T_s - T_c$ remains about 200 K, as may be obtained more accurately by the definition of Δ_c .

Effect of Different Temperatures:

To study the effect of different temperatures of the approaching streams on the values of Δ_c and Δ_1 , it is convenient to consider first the physically relevant limiting case $L_H \ll 1$. We show below that, with the inviscid potential solution adopted for the flow field, the shape and location of the bifurcated branch in this case are independent of the fuel stream temperature. Taking the limit $L_H \rightarrow 0$ in Eq. (6) yields the asymptotic frozen profiles $y_{O_{2f}} = 0$, $\theta_f = \theta_\infty$ for $\zeta < 0$, and $y_{O_2} = 1$, $\theta_f = 0$ for $\zeta > 0$. The shape of these functions agrees with the fact that the transverse coordinate of the mixing layer, ζ , has been nondimensionalized with the characteristic diffusion length corresponding to H . In the limit $L_H \rightarrow 0$, the hydrogen diffusivity is much larger than the oxygen and thermal diffusivities. Therefore, diffusion of O_2 and heat conduction take place in a thin layer located around $\zeta = 0$. The oxidizer is unable to reach the fuel side of the mixing layer. The reaction is frozen for $\zeta < 0$ because of the absence of oxygen. The values of Δ_c and Δ_1 are, therefore, only determined by what occurs on the oxidizer side of the mixing layer and become independent of the temperature of the fuel stream. At this point, it becomes clear that T_∞ is the most relevant temperature for the ignition problem and is properly selected to nondimensionalize the equations. The analysis above indicates that, when the temperatures of the approaching streams are different, Fig. 2 still gives the critical Damköhler number for ignition and the slope of the bifurcated branch, provided $L_H \ll 1$.

To study departures from this result, we consider the case $T_\infty \gg T_c$, i.e., $\gamma \ll 1$, so that $\Delta_c = \Delta_0$ and the effect of $T_\infty < T_s$ reduces to the appearance of an additional factor $\exp(\beta_1 \theta_f)$ multiplying the right-hand side of Eqs. (8) through (10). Figure 3 shows the ratio $\Delta_c/(\Delta_c)_0$, in which $(\Delta_c)_0$ is the value of Δ_c corresponding to $\theta_\infty = 0$. As can be seen from this graph, although Fig. 2 loses accuracy as L_H increases, it still gives a reasonably good approximation for the critical Damköhler number for ignition.

Solution for Small L_H :

In the limit $L_H \ll 1$, Eq. (8), modified to account for different stream temperatures, can be solved in the case $T_\infty \gg T_c$ to determine Δ_c as an asymptotic

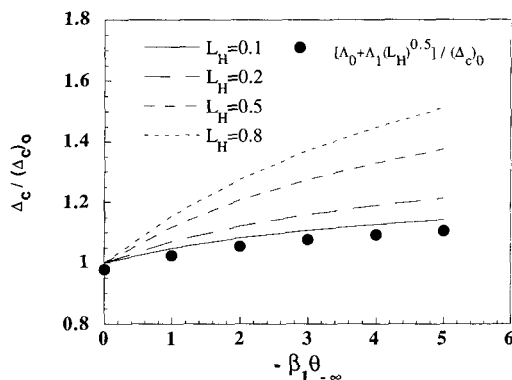


FIG. 3. Effect of the fuel stream temperature on the critical Damköhler number.

expansion in the small parameter $\sqrt{L_H}$ of the form $\Delta_c = \Delta_0 + \sqrt{L_H} \Delta_1 + L_H \Delta_2 + \dots$. In this limit, the solution can be found by dividing the flow field into three distinct layers, two outer layers on the fuel and oxidizer sides with characteristic nondimensional length of order unity and an inner layer, located around $\zeta = 0$, with characteristic nondimensional length of order $\sqrt{L_H}$. Equation (8) must be solved separately in those three layers, and the value of Δ_c can then be found by matching the different solutions. Let y_l , y_r , and y_i denote the value of y_{H0} in the left outer, right outer, and inner layer, respectively. If one neglects exponentially small terms in Eq. (8), the solutions in the outer layers can be shown to be $y_l = 2[1 - 1/2 \operatorname{erfc}(\zeta/\sqrt{2})]$ and $y_r = C \exp(-\zeta^2/4) U(1/2 - \Delta_c, \zeta)$, where U is the Whittaker's function as defined in Ref. 14. In deriving these expressions, the boundary conditions of Eq. (8) have been used, and the arbitrary value of y_i at $\zeta = 0$ has been chosen to be unity. The value of the constant C must be determined from the matching conditions with the inner layer as an expansion in the small parameter $\sqrt{L_H}$.

To describe this inner layer, a stretched coordinate $\zeta/\sqrt{L_H}$ must be introduced, and the value of y_i has to be expanded in the form $y_i = (y_i)_0 + \sqrt{L_H}(y_i)_1 + \dots$. This kind of formulation results in a set of equations for the inner layer that must be solved order by order by matching with the solutions for the outer layers given above. Solution to the first three orders provides expressions for Δ_0 and Δ_1 , which can be shown to be

$$\sqrt{\pi} = - \frac{\Gamma\left(\frac{1}{2} - \frac{\Delta_0}{2}\right)}{\Gamma\left(1 - \frac{\Delta_0}{2}\right)} \quad (14)$$

$$A_1 = \frac{\sqrt{2\pi} A_0}{\Psi\left(\frac{1}{2} - \frac{A_0}{2}\right) - \Psi\left(1 - \frac{A_0}{2}\right)} \cdot \int_0^\infty F\left(\frac{1}{2} \operatorname{erfc}\left(\frac{t}{\sqrt{2}}\right), \beta_1 \theta_f\right) dt \quad (15)$$

where Γ and Ψ are, respectively, the gamma and digamma functions and F is defined as $F(x_1, x_2) = 1 + (x_1 - 1) \exp(x_1 x_2) - x_1 \exp[(1 - x_1)x_2]$. It can be shown that the only value of A_0 that is a solution of Eq. (14) and also satisfies the additional constraint $U(1/2 - A_c, \zeta) > 0$ is given approximately by $A_0 = 1.4251$. Comparison of the two-term asymptotic expansion for A_c with the result obtained by numerical integration is shown in Fig. 3 for the case $L_H = 0.1$. As can be seen, retaining two terms in the expansion suffices to give a good approximation in this case.

The value of A_1 becomes zero when the two approaching streams have the same temperature. In that case, the analysis, which is valid for $\gamma \neq 0$, must be carried to a higher order if the effect of $L_H \neq 0$ is to be taken into account. The next two terms in the expansion for A_0 were found to be $A_2 = 2 A_0 [\Psi(1/2 - A_0/2) - \Psi(1 - A_0/2)] \approx 0.3866$ and $A_3 = -(\sqrt{2}/3) A_0 A_2 \approx -0.2597$. The expansion $A_0 = A_0 + L_H A_2 + L_H^2 A_3$ gives the value of A_0 for equal stream temperatures within 1% accuracy for values of L_H as large as 0.45.

Nonlinear Analysis of a Simplified Model

Although a simple weakly nonlinear analysis suffices to determine the dependence of the shape of the ignited branch on the different parameters present in the problem, calculation of the solution away from the bifurcation point involves numerical integration of a four-equation boundary-value problem. A significant simplification is obtained if we restrict our attention to the case $T_\infty \gg T_c$, i.e., $\gamma \ll 1$, and also assume that the Lewis numbers of all species present in the mixture are unity. This assumption is clearly inaccurate for hydrogen, whose diffusivity is much higher than that of heat or oxygen. Therefore, the results presented below are not intended to be accurate but rather qualitatively correct. The results would also be quantitatively correct if the chain-branching species were O or OH instead of H.

In this case, the problem reduces to that of solving the differential equation

$$\zeta \frac{\partial y_H}{\partial \zeta} + \frac{\partial^2 y_H}{\partial \zeta^2} = -\Delta \exp(\beta_1 \theta_f) \exp(\beta_1 q_1 y_H) (y_{O_2f} - s y_H) y_H \quad (16)$$

subject to $y_H(-\infty) = 0$, $y_H(\zeta_d) = 1/6 \operatorname{erfc}(\zeta_d/\sqrt{2})$ and $dy_H/d\zeta(\zeta_d) = -(1/6)\sqrt{2/\pi} \exp(-\zeta_d^2/2)$. In de-

termining Eq. (16), the boundary conditions of Eqs. (1) through (3) have been used to integrate linear combinations of Eqs. (1) and (2) and of Eqs. (1) and (3), respectively. A similar linear combination of Eqs. (1) and (4) was integrated to obtain $y_{H_2} + 3y_H = 1/2 \operatorname{erfc}(\zeta/\sqrt{2})$, which was used when determining the boundary conditions at $\zeta = \zeta_d$. The ignited solutions of this problem were obtained by numerical integration using a simple shooting method.⁹ For a given value of ζ_d , integration of the equation starting from $\zeta = \zeta_d$ determines a unique value of Δ for which the solution is positive everywhere and also satisfies the boundary condition at $-\infty$. Different solutions obtained for increasing values of the parameter $\Omega = \beta_1 q_1/s$ are shown in Fig. 4. The bifurcated branch becomes subcritical when the value of Ω exceeds the Ω_s predicted by the weakly nonlinear analysis. Away from the bifurcation point, the consumption of O₂ eventually takes over, and the subcritical bifurcated branches turn around, beginning to reproduce the S-shaped curve typical of diffusion flames.

The asymptotic value approached by the bifurcated branch for large values of Δ was also determined. Since the model employed accounts for H₂ depletion, the limit $\Delta \rightarrow \infty$ consistently gives the flame-sheet approximation. In the limit $\Delta \rightarrow \infty$, H₂ and O₂ do not coexist, and the chemical reaction is confined in an infinitesimally thin layer located at $\zeta = \zeta_d$. The location of the flame is obtained from the jump condition at the flame sheet,

⁹We can anticipate the results of the numerical integration of Eq. (16) by using a simple lumped approximation for the equation. In this approximation, attention is restricted to the reaction region, where $y_H \sim y_{H_{\max}}$. The differential operator on the left-hand side of the equation, which represents the loss of radicals by diffusion, is replaced by the term $-ay_{H_{\max}}$, with a of order unity, and the functions y_{O_2f} and $\exp(\beta_1 \theta_f)$ by their values in the reaction region, y'_{O_2f} and $\exp(\beta_1 \theta'_f)$, both quantities of order unity. With these approximations, Eq. (16) reduces to the simple algebraic equation

$$ay_{H_{\max}} = \Delta \exp(\beta_1 \theta'_f) \exp(\beta_1 q_1 y_{H_{\max}}) (y'_{O_2f} - s y_{H_{\max}}) y_{H_{\max}}$$

This equation admits two different solutions, $y_{H_{\max}} = 0$ and $\Delta = a[y'_{O_2f} \exp(\beta_1 \theta'_f)]^{-1} \exp(\beta_1 q_1 y_{H_{\max}}) [1 - (s/y'_{O_2f}) y_{H_{\max}}]^{-1}$, corresponding to the frozen and ignited solutions, respectively. Some characteristics of the ignited branch that appear in the numerical results are summarized here. The ignited branch departs from the frozen one at a critical value of the Damköhler number of order unity given by $[y'_{O_2f} \exp(\beta_1 \theta'_f)]^{-1} a$. By linearizing the expression for the ignited branch for small values of $y_{H_{\max}}$, it can be seen that the bifurcation is supercritical as long as $\beta_1 q_1/s < [y'_{O_2f}]^{-1}$, again a quantity of order unity. Away from the bifurcation point, the ignited branch evolves so that the Damköhler number becomes infinite as $y_{H_{\max}}$ approaches a value of order s^{-1} .

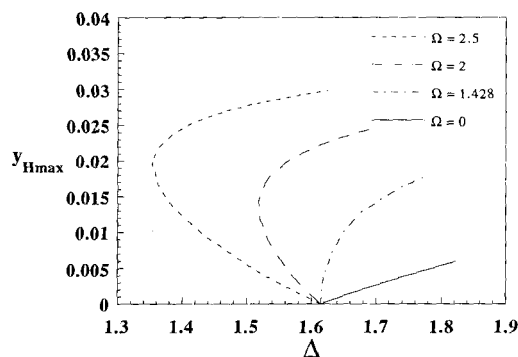


FIG. 4. Effect of heat release on the shape of the ignition branch for $s = 20$ and $L_H = 1$.

$$\left[s \frac{\partial y_H}{\partial \zeta} + \frac{\partial y_{O_2}}{\partial \zeta} \right]_{\zeta_d} = 0 \quad (17)$$

which can be used to find the asymptotic values of ζ_d and $y_{H_{\max}}$,

$$\zeta_d = \sqrt{2} \operatorname{erfc}^{-1} \left(\frac{6}{s+3} \right), \quad y_{H_{\max}} = \frac{1}{s+3} \quad (18)$$

where erfc^{-1} is the inverse of the complementary error function.

Discussion and Conclusions

We have seen how the chain-branching process producing hydrogen atoms controls the high-temperature ignition in strained mixing layers of hydrogen and air. The resultant chain-branching process can be described by a two-step reduced kinetic mechanism. It was shown that, in the limit $L_H \rightarrow 0$, the ignition process becomes independent of the fuel-stream temperature and is mainly controlled by the oxidizer-stream temperature. Small changes to this result are expected if a more exact description of the flow field is implemented in the analysis.

Because of the particular kinetic mechanism that controls the process, ignition does not take place as a smooth turning point, and three distinctive behaviors were identified. For values of T_∞ above crossover, the solution consists of a bifurcated branch departing from the frozen solution at a critical value of the Damköhler number, Δ_c . From a linear analysis, Δ_c was found as the solution for the eigenvalue in an eigenvalue problem. Also, the slope of the ignition branch in the vicinity of the bifurcation point was calculated as part of the solution, and a limiting temperature T_s was obtained. The bifurcated solution

was found for $T_\infty > T_s$ to be supercritical. This corresponds to a smooth transition from a frozen solution to a diffusion flame as the Damköhler number increases. This lack of abrupt ignition for $T_\infty > T_s$ was also observed in the numerical solutions [8,9]. The large heat release associated with the recombination changes the character of the bifurcation to subcritical when $T_\infty = T_s$, and an abrupt type of ignition is obtained below this temperature.

Because of the chain-terminating effect of the principal heat-release step, the value of Δ_c increases significantly as T_∞ approaches T_c , in qualitative agreement with results of previous numerical studies [8,9]. At crossover, Δ_c becomes infinite; i.e., the critical strain rate becomes zero, and below this temperature, the solution consists of a C-shaped curve unconnected to the frozen solution.

Although the kinetic model employed qualitatively reproduces the numerical results shown in previous studies [8,9], further quantitative comparisons with numerical and experimental work are required to test the parametric results presented here. In addition, further analytical study must be given to conditions with $T_\infty \ll T_c$, where a thermal-explosion character is anticipated, before simple results can be presented that can be used widely in engineering practice.

Acknowledgment

This work was supported by the National Science Foundation through Grant No. CTS-92-14888.

REFERENCES

1. Treviño, C., *Progress in Astronautics and Aeronautics*, AIAA Inc., New York, 1991, Vol. 131, pp. 19–43.
2. Baulch, D. L., Drysdale, D. D., Horne, D. G., and Lloyd, A. C., *Evaluated Kinetic Data for High Temperature Reactions*, Butterworths, London, 1972, Vol. 1.
3. Dixon-Lewis, G., and Williams, D. J., in *Comprehensive Chemical Kinetics* (C. H. Bamford and C. F. H. Tipper Eds.), Elsevier, Oxford, UK, 1977, Vol. 17, pp. 109–144.
4. Warnatz, J., in *Combustion Chemistry* (W. C. Gardiner, Ed.), Springer, New York, 1984, pp. 197–360.
5. Baulch, D. L., Cobos, C. J., Cox, R. A., Esser, C., Frank, P., Just, Th., Kerr, J. A., Philling, M. J., Troe, J., Walker, R. W., and Warnatz, J., *J. Phys. Chem. Ref. Data* 21:411–736 (1992).
6. Clavin, P., *Prog. Energy Combust. Sci.* 11:51 (1985).
7. Treviño, C., and Méndez, F., *Combust. Sci. Technol.* 78:197–216 (1991).
8. Balakrishnan, G., Smooke, M. D., and Williams, F. A., "A Numerical Investigation of Extinction and Ignition Limits in Laminar Nonpremixed Counterflowing Hy-

- drogen-Air Streams for Both Elementary and Reduced Chemistry," unpublished, 1993.
9. Darabiha, N., and Candel, S., *Combust. Sci. Technol.* 86:67–85 (1993).
 10. Niioka, T., *Combust. Flame* 76:143–149 (1988).
 11. Treviño, C., and Liñán, A., "High Temperature Ignition of Hydrogen in Mixing Layers," paper presented at the International Colloquium on Dynamics of Explosions and Reactive Systems in Coimbra, Portugal, August 1–4, 1993.
 12. Liñán, A., *Acta Astronaut.* 1:1007–1039 (1974).
 13. Seshadri, K., Peters, N., and Williams, F. A., *Combust. Flame* 96:407–427 (1994).
 14. Abramowitz, M., and Stegun, A., *Handbook of Mathematical Functions*, Dover, New York, 1965, pp. 686–689.